

# Statistical Amplitude Scale Estimation for Quantization-based Watermarking

Ivo D. Shterev, Inald L. Lagendijk, and Richard Heusdens

Delft University of Technology, Mekelweg 4, 2628 CD, Delft, The Netherlands

## ABSTRACT

Quantization-based watermarking schemes are vulnerable to amplitude scaling. Therefore the scaling factor has to be accounted for either at the encoder, or at the decoder, prior to watermark decoding. In this paper we derive the marginal probability density model for the watermarked and attacked data, when the attack channel consists of amplitude scaling followed by additive noise. The encoder is Quantization Index Modulation with Distortion Compensation. Based on this model we obtain two estimation procedures for the scale parameter. The first approach is based on Fourier Analysis of the PDF. The estimation of the scaling parameter relies on the structure of the received data. The second approach that we obtain is the Maximum Likelihood estimator of the scaling factor. We study the performance of the estimation procedures theoretically and experimentally with real audio signals, and compare them to other well known approaches for amplitude scale estimation in the literature.

**Keywords:** quantization, characteristic functions, maximum likelihood estimation, watermarking

## 1. INTRODUCTION

Watermarking schemes based on Quantization Theory have recently emerged as a result of Information Theoretic analysis<sup>1,2</sup>. These schemes prove to perform better than the well known spread spectrum watermarking in the context of additive attacks. However, the resulting watermarking schemes fail to perform well for a number of important non-additive attacks (operations). One such operation is amplitude scaling which is a common operation in many applications, such as audio play out and recording. Another application is Digital Audio Broadcasting (*DAB*), where amplitude scaling is even more complex, because different frequency bands are scaled (filtered) with different factors. Nonlinear scaling such as gamma correction can be seen in image processing applications. Quantization-based watermarking schemes are vulnerable against amplitude scaling. The reason for this is the fact that in order to assist the structured decoder, a Maximum A Posteriori (*MAP*) estimation of the codeword used in the embedding stage is needed. Therefore, the amplitude scaling factor has to be known at the detection side for reliable codeword estimation.

Two approaches have been proposed in the literature to combat the scaling attack. One of them is based on estimating the scaling factors using the histogram of the received data. Once a good estimate is obtained, the scaling factors can be accounted for by dividing the received data by the estimated scaling factors, or by an appropriate modification of the watermark detector.<sup>3</sup> Another approach is based on optimized for the scaling attack codes<sup>4,5</sup>, such as modified trellis codes.<sup>6</sup>

In this paper we derive the probability density model of the received watermarked and attacked data when the encoder is Quantization Index Modulation (*QIM*) with distortion compensation (*DC*). Based on this model we derive two approaches for estimation of amplitude scaling modifications. In section 2, a mathematical model of the problem is introduced. In section 3, the model of the probability density function (*PDF*) of the received data is derived. In section 4.1, a procedure based on Fourier Analysis is examined, and experimental validation is given in section 4.2. In section 5.1, the maximum likelihood estimator is described and experimental validations are given in section 5.2. In section 6.1 we compare the two proposed estimation techniques, and in section 6.2, we describe the case when different messages are embedded. Finally, conclusions and discussion are presented in section 7.

---

Further author information: (Send correspondence to Ivo D. Shterev)  
Ivo D. Shterev: E-mail: i.shterev@ewi.tudelft.nl

## 2. PROBLEM FORMULATION

The general model of the problem that we consider is shown in Figure 1 together with the watermark encoder. The dither which is most schemes is used for security purposes is assumed absent, and the quantizer used is an ordinary scalar quantizer. In Figure 1,  $W$  is the embedded message,  $\tilde{X}$  is the host data with variance  $\sigma^2$ ,  $X$  is the watermarked data,  $U$  is the codeword used at the embedding stage,  $\beta$  is the scaling factor that we want to estimate,  $N \sim \mathcal{N}(0, \sigma_N^2)$  is the additive part of the attack channel, independent of the watermarked data,  $Y$  is the attacked data, and  $\hat{W}$  is the estimated message. The watermark encoder implements two shifted uniform quantizers with step size  $\Delta$  and shift  $\frac{\Delta}{2}$  (see<sup>7</sup>). The distortion that the encoder introduces is equal to that of the quantizer only and is given as  $\sigma_\Delta^2 = \frac{\Delta^2}{12}$ . The quantity  $\alpha = \frac{\sigma_\Delta^2}{\sigma_\Delta^2 + \sigma_N^2}$  is known from.<sup>8</sup> Throughout the paper we will assume scalar random variables.

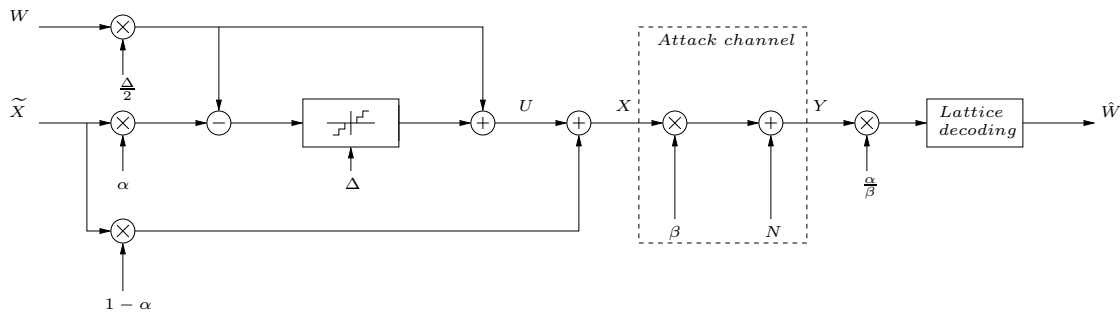


**Figure 1.** General model for the amplitude scaling problem.

In this paper we will mostly concentrate on modelling the encoding process, because we are interested in estimation of  $\beta$ . Once  $\beta$  is estimated, the decoder will scale by  $\frac{\alpha}{\beta}$  and apply lattice decoding to the result as shown in Figure 1.

## 3. PDF MODEL FOR THE WATERMARKED DATA

In this section we will derive the mathematical model for the watermarked data and attacked data, when the attack channel consists of amplitude scaling followed by additive noise. Then we will give several examples illustrating the structure of the different PDFs.

The PDF of the watermarked data can be written as:

$$f_X(x) = f_{X|W}(x|w=0)P(W=0) + f_{X|W}(x|w=1)P(W=1) \quad (1)$$

where  $P(W=0)$  and  $P(W=1)$  are the probabilities of occurrence of bit 0 and 1 respectively, and  $f_{X|W}(x|w=0)$  and  $f_{X|W}(x|w=1)$  are the marginal PDFs of the watermarked data corresponding to  $W=0$  and  $W=1$  respectively.

First we will derive  $f_{X|W}(x|w=0)$ . The derivation of  $f_{X|W}(x|w=1)$  will follow using similar reasoning.

Lets consider the case when the input to the quantizer is in the  $k$  quantization sell, (i.e. the output of the quantizer is  $U=k\Delta$ ), where  $k$  is an arbitrary integer. From Figure 1 this case is equivalent in terms of  $\tilde{X}$  to:

$$\frac{\Delta}{\alpha}(k - \frac{1}{2}) < \tilde{X} < \frac{\Delta}{\alpha}(k + \frac{1}{2}) \quad (2)$$

The probability of the watermarked data for this particular case can be expressed as:

$$f'_{X|W}(x|w=0) = \frac{1}{1-\alpha} f_{\tilde{X}}(\frac{x-k\Delta}{1-\alpha}) I_{A_{k|w=0}}(x) \quad (3)$$

where  $I_{A_{k|w=0}}(x)$  denotes the indicator function of the set  $A_{k|w=0}$  defined as:

$$I_{A_{k|w=0}}(x) = \begin{cases} 1 & \text{if } x \in A_{k|w=0} \\ 0 & \text{if } x \notin A_{k|w=0} \end{cases} \quad (4)$$

and

$$A_{k|w=0}(x) = \left\{ x : \frac{\Delta}{\alpha} \left( k - \frac{1-\alpha}{2} \right) < X < \frac{\Delta}{\alpha} \left( k + \frac{1-\alpha}{2} \right) \right\} \quad (5)$$

Generalizing for all  $k$ , we can write:

$$f_{X|W}(x|w=0) = \sum_{k=-\infty}^{\infty} \frac{1}{1-\alpha} f_{\tilde{X}} \left( \frac{x-k\Delta}{1-\alpha} \right) I_{A_{k|w=0}}(x) \quad (6)$$

In the same fashion we can express the PDF of the watermarked data for  $W = 1$  as:

$$f_{X|W}(x|w=1) = \sum_{k=-\infty}^{\infty} \frac{1}{1-\alpha} f_{\tilde{X}} \left( \frac{x - \frac{2k+1}{2}\Delta}{1-\alpha} \right) I_{A_{k|w=1}}(x) \quad (7)$$

where

$$I_{A_{k|w=1}}(x) = \left\{ x : \frac{\Delta}{\alpha} \left( k + \frac{\alpha}{2} \right) < X < \frac{\Delta}{\alpha} \left( k + \frac{2-\alpha}{2} \right) \right\} \quad (8)$$

Substituting with (5) and (6) in (1), we can get:

$$\begin{aligned} f_X(x) &= \frac{1}{1-\alpha} \sum_{k=-\infty}^{\infty} \left[ f_{\tilde{X}} \left( \frac{x-k\Delta}{1-\alpha} \right) I_{A_{k|w=0}}(x) P(W=0) \right. \\ &\quad \left. + f_{\tilde{X}} \left( \frac{x - \frac{2k+1}{2}\Delta}{1-\alpha} \right) I_{A_{k|w=1}}(x) P(W=1) \right] \end{aligned} \quad (9)$$

Taking the scaling factor  $\beta$  and the additive part  $N$  into account, we can write the probability of the received data as:

$$\begin{aligned} f_Y(x|\beta) &= f_N(x) * \frac{1}{\beta(1-\alpha)} \sum_{k=-\infty}^{\infty} \left[ f_{\tilde{X}} \left( \frac{x-k\beta\Delta}{\beta(1-\alpha)} \right) I_{A_{k|\beta,w=0}(x)}(x) P(W=0) \right. \\ &\quad \left. + f_{\tilde{X}} \left( \frac{x - \frac{2k+1}{2}\beta\Delta}{1-\alpha} \right) I_{A_{k|\beta,w=1}(x)}(x) P(W=1) \right] \end{aligned} \quad (10)$$

where  $*$  denotes convolution, and

$$A_{k|\beta,w=0}(x) = \left\{ x : \frac{\Delta\beta}{\alpha} \left( k - \frac{1-\alpha}{2} \right) < X < \frac{\Delta\beta}{\alpha} \left( k + \frac{1-\alpha}{2} \right) \right\} \quad (11)$$

$$A_{k|\beta,w=1}(x) = \left\{ x : \frac{\Delta\beta}{\alpha} \left( k + \frac{\alpha}{2} \right) < X < \frac{\Delta\beta}{\alpha} \left( k + \frac{2-\alpha}{2} \right) \right\} \quad (12)$$

Throughout the paper, for simplicity we will assume that  $P(W=0) = 1, P(W=1) = 0$ , and therefore working only with the first term of (10)\*. An extension to the general case when the encoder embeds zeros and ones with a specified probability is straightforward, using the complete expression (10). The quantity  $\frac{\Delta\beta}{\alpha}$  in (11) indicates that watermark decoding can be done directly (without MAP estimation) by applying lattice decoding with a step size  $\frac{\alpha}{\beta}\Delta$ , therefore signifying the importance of knowing beta at detection side. In Figure 2, a plot of PDF models for the host, watermarked, and attacked data is shown with Gaussian sources as host and attack signals, and for different values of the ratio  $\frac{\sigma_N^2}{\sigma_\Delta^2}$ . The structure in the PDF of the watermarked data is clearly observable and will be the main tool in developing the estimation procedures in the next sections. We can also see that the the width of the nonzero regions in the probability of the watermarked data changes with changing the variance  $\sigma_N^2$  (since the encoder knows the channel statistics), and later it will be shown that this turns out to play a favorable role in the estimation approach based on Fourier Analysis.

---

\*We will return to the issue  $P(W=0), P(W=1) \neq 0$  in section 6.2.

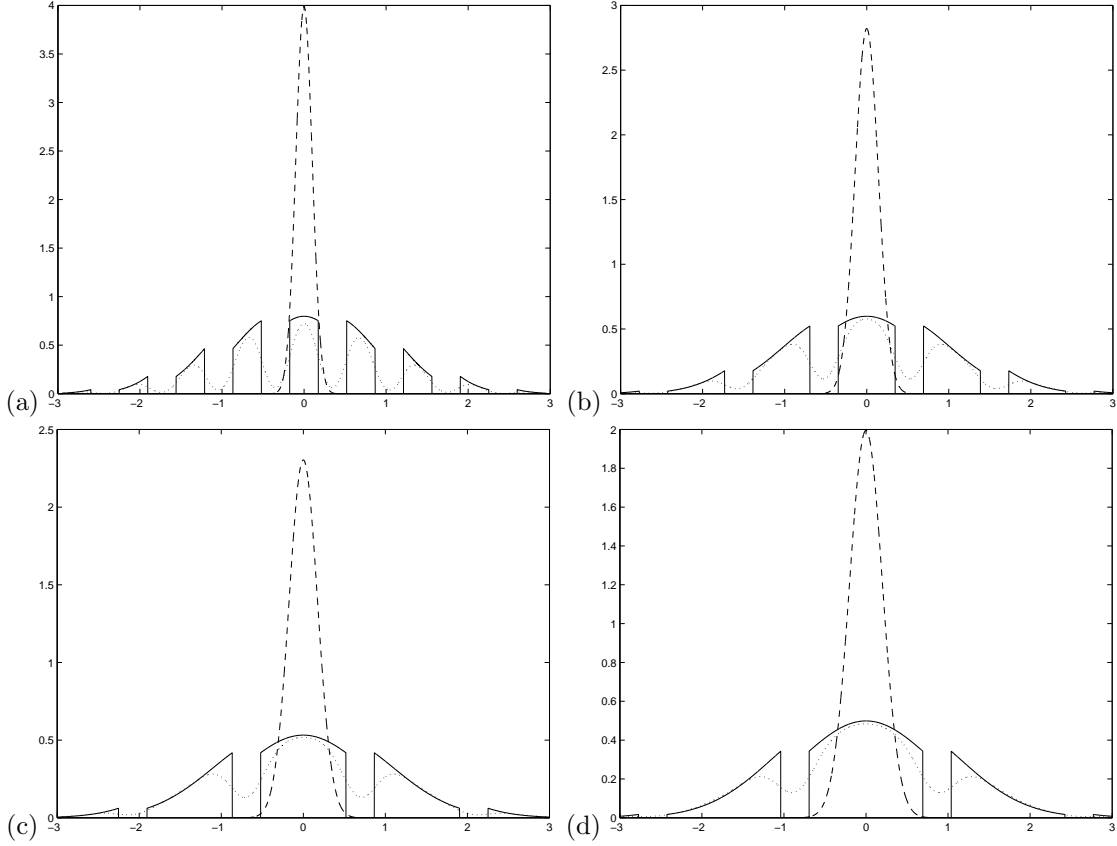


**Figure 2.** Plot of PDF models for Gaussian sources as host and attack signals. The solid curve is the pdf of  $X \sim \mathcal{N}(0, \sigma^2)$ , the dashed curve is the pdf of  $N \sim \mathcal{N}(0, \sigma_N^2)$ , the dotted curve is the pdf of  $Y$  as given by the first term of (11). (a)  $\sigma_N^2 = \sigma_\Delta^2$ , (b)  $\sigma_N^2 = 2\sigma_\Delta^2$ , (c)  $\sigma_N^2 = 3\sigma_\Delta^2$ , (d)  $\sigma_N^2 = 4\sigma_\Delta^2$ . In all cases  $\sigma_\Delta^2 = \frac{\sigma^2}{100}$ , and  $\beta = 1$ .

## 4. ESTIMATION OF AMPLITUDE SCALING BASED ON FOURIER ANALYSIS

### 4.1. Estimation

In this section we derive a procedure for scale estimation based on Fourier Analysis of the expression (10). A similar procedure was derived by Eggers<sup>3</sup> for the watermark encoding function  $X = (1 - \alpha^*)\tilde{X} + \alpha^*Q(\tilde{X})$  in the presence of dither, where  $Q(\cdot)$  denotes uniform quantization. In<sup>3</sup> the authors choose the optimal values for the quantizer step size and the coefficient  $\alpha^*$  numerically.<sup>9</sup> We noticed, though that there is no significant difference in performance between our procedure based on Fourier analysis and that described in<sup>3</sup>.

We will need to define the characteristic function (c.f.) of a random variable  $X$  with p.d.f.  $f_X(x)$  as:

$$\Phi_X(\omega) = \int_{-\infty}^{+\infty} f_X(x)e^{i\omega x} dx \quad (13)$$

From Eq. (11) and also from Figure 2 we can see that  $f_{X|W}(x|w=0)$  has a regular structure of discontinuity and continuity regions with width of  $\Delta\beta$  and  $\Delta\beta\frac{\sigma_N^2}{\sigma_\Delta^2}$  respectively. The total distance between the discontinuities is  $\Delta\beta + \Delta\beta\frac{\sigma_N^2}{\sigma_\Delta^2} = \frac{\Delta\beta}{\alpha}$ . Therefore  $\Phi_X(\omega)$  will have a periodic-like structure with a period  $2\pi\frac{\alpha}{\Delta\beta}$ . Observing (11), we can say that the periodicity of  $\Phi_X(\omega)$  will not change if we embed only ones, i.e.  $P(W=1)=1$ , showing the advantage of working in the Fourier domain. From (10) it follows that the c.f. of the received data can be written as

$$\Phi_Y(\omega) = \Phi_X(\omega)\Phi_N(\omega) \quad (14)$$

where  $\Phi_N(\omega)$  is the c.f. of  $N$ . In the estimation procedure we will need to estimate the periodicity  $2\pi \frac{\alpha}{\Delta\beta}$  from  $\Phi_Y(\omega)$ , which due to the additive part in the attack channel will be disturbed in a degree depending on the strength of  $N$  (see Figure 3).

## 4.2. Practical Aspects of the Procedure based on Fourier Analysis

An illustration of characteristic functions for host, watermarked, and attacked data, for Gaussian sources and different ratios of  $\frac{\sigma_N^2}{\sigma_\Delta^2}$  is shown in Figure 3. The first dominating peak away from zero frequency is always at  $\omega = 2\pi \frac{\alpha}{\Delta\beta}$ .

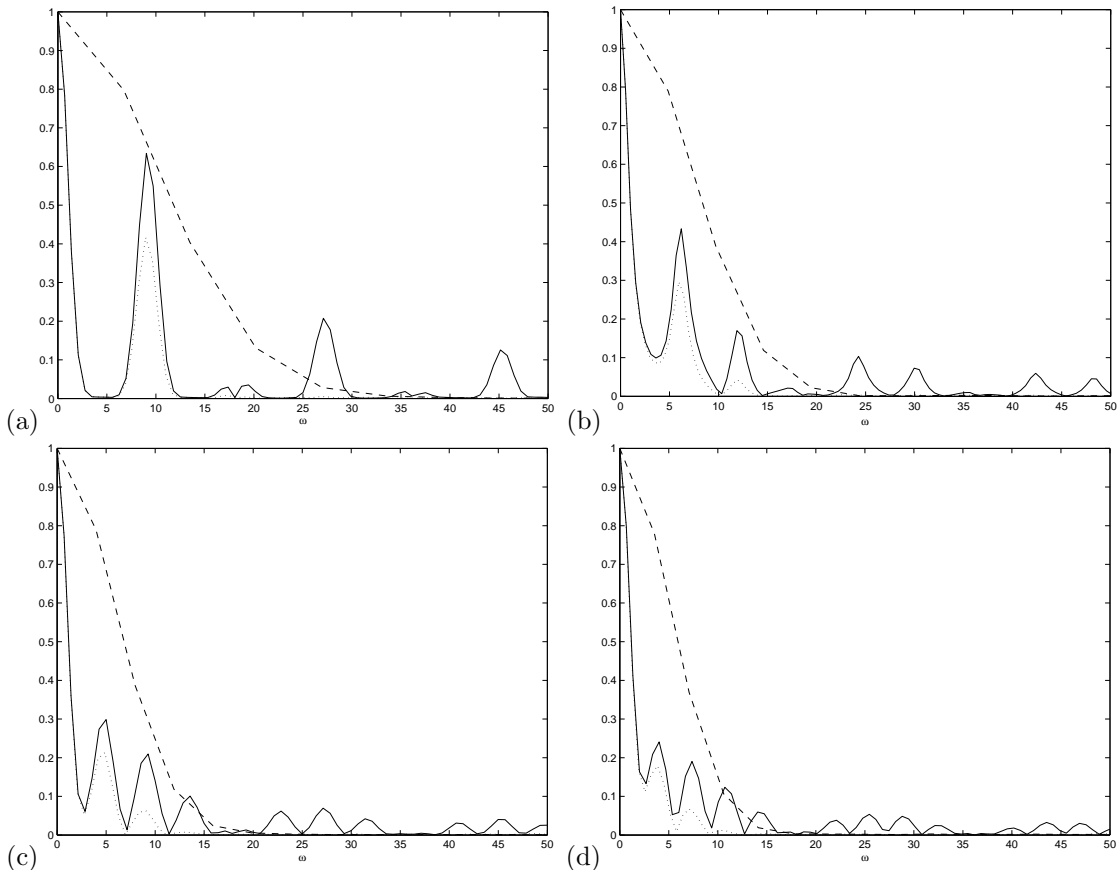


**Figure 3.** Plot of c.f.s for Gaussian sources and different ratios of  $\frac{\sigma_N^2}{\sigma_\Delta^2}$ . The solid curve is  $\Phi_X(\omega)$ , the dashed curve is  $\Phi_N(\omega)$ , and the dotted line is  $\Phi_Y(\omega)$ . (a)  $\frac{\sigma_N^2}{\sigma_\Delta^2} = 1$ , (b)  $\frac{\sigma_N^2}{\sigma_\Delta^2} = 2$ , (c)  $\frac{\sigma_N^2}{\sigma_\Delta^2} = 3$ , (d)  $\frac{\sigma_N^2}{\sigma_\Delta^2} = 4$ .

There are two interesting features of the encoder that are due to the presence of  $\alpha$  in the periodicity of  $\Phi_X(\omega)$ . The first one improves the estimation robustness, while the second one hampers it. Increasing  $\sigma_N^2$ , the slope of  $\Phi_N(\omega)$  becomes steeper, and since  $\Phi_N(\omega) \leq \Phi_N(0) = 1$  for every  $\omega$  (which is true for every valid c.f., see<sup>10</sup>), we can say that for big ratios  $\frac{\sigma_N^2}{\sigma_\Delta^2}$ , only those peaks of  $\Phi_X(\omega)$  that are nearer to  $\omega = 0$  will survive. Fortunately increasing  $\frac{\sigma_N^2}{\sigma_\Delta^2}$  will also decrease  $\alpha$  and the peaks of  $\Phi_X(\omega)$  will be shifted towards lower frequencies, countering the effect of increasing  $\sigma_N^2$ . The negative impact of  $\alpha$  consists of the fact that with increasing the ratio  $\frac{\sigma_N^2}{\sigma_\Delta^2}$ , a bigger part of the host signal will pass through the  $(1 - \alpha)\tilde{X}$  branch, therefore reducing the part that passes through the quantizer. As a result the zero regions in the PDF of the watermarked data will tend to disappear

as  $\frac{\sigma_N^2}{\sigma_\Delta^2}$  increases, the peaks in  $\Phi_X(\omega)$  will become flatter (even before multiplying with  $\Phi_N(\omega)$ ) as illustrated in Figure 3, from which it would be more difficult to estimate the scaling factor. However, experiments showed that the positive feature prevails and knowing the statistics at the encoder side gives better results than the case of *QIM*.

## 5. MAXIMUM LIKELIHOOD ESTIMATION OF AMPLITUDE SCALING

### 5.1. Description

In this section we will derive the Maximum Likelihood (*ML*) functional of  $\beta$  and study its properties. A derivation of an analytical expression for this method is quite tedious and in most cases is not possible. That is why we have to constrain ourselves to working with convolution of *PDFs*.

The *ML* estimator of  $\beta$  can be written as:

$$\hat{\beta} = \arg \max_{\beta} f_Y(y|\beta) \quad (15)$$

We will assume that the samples of the received data are independent, for which we can write the joint *PDF* of the received data as a product of the individual densities, i.e.  $f_Y(y) = f_Y(y_1)f_Y(y_2)\dots f_Y(y_n)$ , where  $n$  is the number of available samples. We note however that such an assumption may result in a source of substantial loss for real audio signals, exhibiting high correlation between the samples. Expanding Eq. (15), we get:

$$\begin{aligned} \hat{\beta} &= \arg \max_{\beta} f_Y(y_1, y_2, \dots, y_n|\beta) \\ &= \arg \max_{\beta} f_Y(y_1|\beta)f_Y(y_2|\beta)\dots f_Y(y_n|\beta) \\ &= \arg \max_{\beta} \sum_i^n \ln f_Y(y_i|\beta) \end{aligned} \quad (16)$$

where the last line follows from the monotonicity of the logarithm.

### 5.2. Practical Aspects of ML estimation

Since it is difficult to further manipulate Eq. (10) for general (even for Gaussian<sup>†</sup>) sources, we perform experiments with Gaussian sources to see the behavior of the *ML* functional  $\sum_i^n \ln f_Y(y_i|\beta)$  as a function of  $\beta$ . In Figure 4(a), curves are shown for different  $\beta$ . In Figure 4(b) we plot the *ML* functional for different ratios  $\frac{\sigma_N^2}{\sigma_\Delta^2}$ . The maximum in the *ML* functional curves indicating the right scaling factor  $\beta$  used in the attack channel is clearly visible in all cases. We can see that around the maximum, the *ML* functional exhibits almost concave behavior.

## 6. DISCUSSION

### 6.1. Comparison between the methods

In this section we compare the performance of the proposed estimation techniques in terms of the ratio  $\frac{\sigma_N^2}{\sigma_\Delta^2}$ , and the number of available signal samples, for different audio signals. Experimental results for the estimation procedure based on Fourier analysis with real audio host signals are shown in Figure 5. It can be seen that reliable estimation of  $\beta$  is possible in the presence of additive noise with ratios up to  $\frac{\sigma_N^2}{\sigma_\Delta^2} = 2$ . From Figure 5(b) it can be seen that for around 1000 signal samples, reliable estimation is also possible.

In Figure 6, the *ML* approach is evaluated with real audio signals (model mismatch) and  $\beta = 1$ . In the experiments the decoder assumes a Laplacian host signal with variance  $\sigma^2 + \sigma_\Delta^2 + \sigma_N^2$ . For the small distortion

---

<sup>†</sup>Because of the discontinuity in  $f_X(x)$  it is difficult to obtain a convenient analytical expression for  $f_Y(x)$  through characteristic functions.

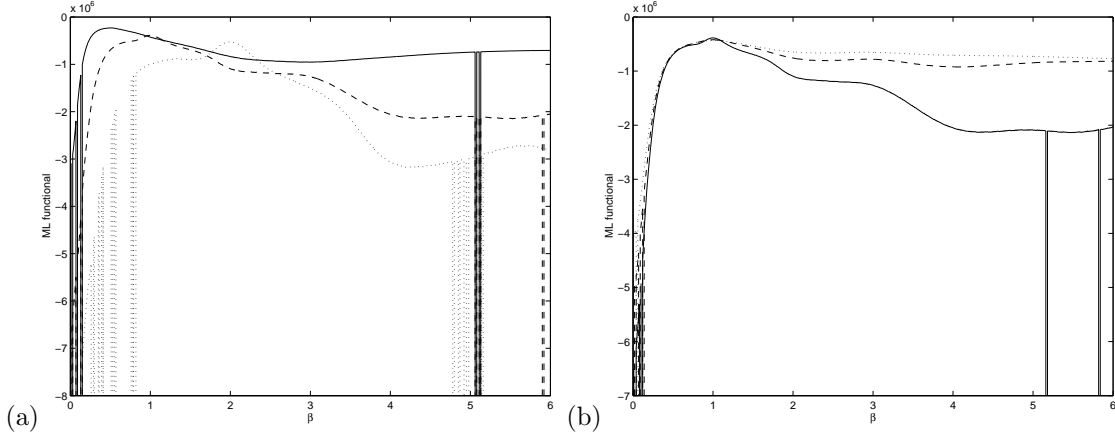


**Figure 4.** Plot of experimental ML functionals with Gaussian sources and  $\frac{\sigma^2}{\sigma_\Delta^2} = 100$ . (a) Different values of  $\beta$ , and fixed  $\sigma_\Delta^2 = \sigma_N^2$ . (b) Different  $\frac{\sigma_N^2}{\sigma_\Delta^2}$ , and  $\beta = 1$ . The solid curve is for  $\sigma_\Delta^2 = \sigma_N^2$ , the dashed curve is for  $\sigma_N^2 = 2\sigma_\Delta^2$ , and the dotted curve is for  $\sigma_N^2 = 3\sigma_\Delta^2$ .

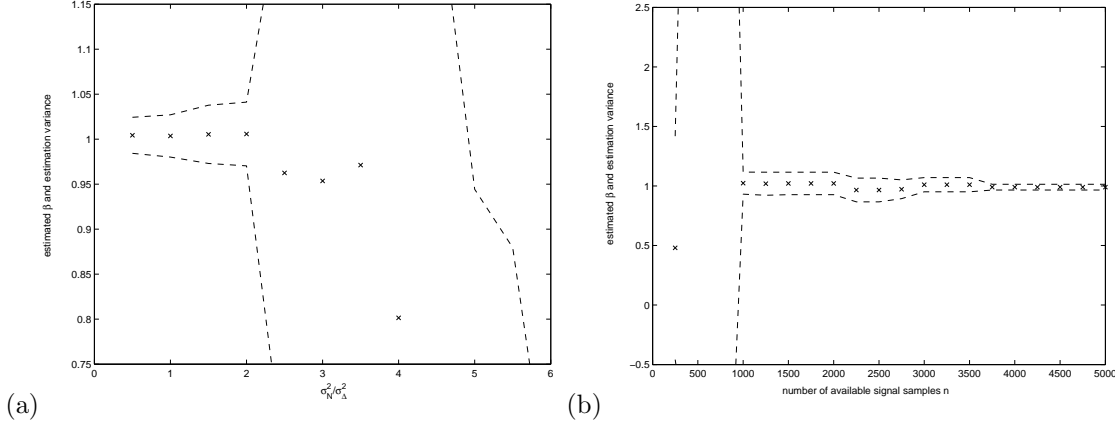


**Figure 5.** Plot of  $\hat{\beta}$  for Fourier-based estimation averaged over different audio signals with fixed ratio  $\frac{\sigma^2}{\sigma_\Delta^2} = 100$ ,  $\beta = 1$ . The crosses represent the estimation mean. The dashed curves represent the variance of the estimation in both directions. (a)  $\frac{\sigma_N^2}{\sigma_\Delta^2}$ , (b) number of available samples, and  $\frac{\sigma_N^2}{\sigma_\Delta^2} = 1$ .

case  $\sigma^2 \gg \sigma_\Delta^2, \sigma_N^2$ ,  $\sigma^2 + \sigma_\Delta^2 + \sigma_N^2 \approx \sigma^2$ . Therefore, in practical applications, guessing the host signal variance at the detection side is not a big issue. In terms of the ratio  $\frac{\sigma_N^2}{\sigma_\Delta^2}$ , the ML approach outperforms the Fourier based approach, especially at high ratios  $\frac{\sigma_N^2}{\sigma_\Delta^2}$ . In terms of the number of available signal samples, it can be seen that reliable estimation of the amplitude scaling factor with the ML approach is possible from around 2500 samples, which is higher than the minimum signal samples needed for estimation with the Fourier based method.

## 6.2. A Note on Different Messages

In this section we discuss the case of imbedding different messages with specified probabilities  $f(W = 0), f(W = 1) \neq 0$  and its influence on the proposed estimation procedures. Since this case will mostly affect the discontinuity of  $f_X(x)$ , we will concentrate on the Fourier based estimation method.

Lets assume that  $f(W = 0) \approx f(W = 1) \approx 0.5$ , or in other words there is a large enough number of zeros and ones in the watermark bitstream. From Equations (11) and (12) we can see that when  $\alpha = 0.5$ , the union of  $A_{k,W=0}(x)$  and  $A_{k,W=1}(x)$  completely covers the real line,  $f_X(x)$  will be absolutely continuous, and there will be

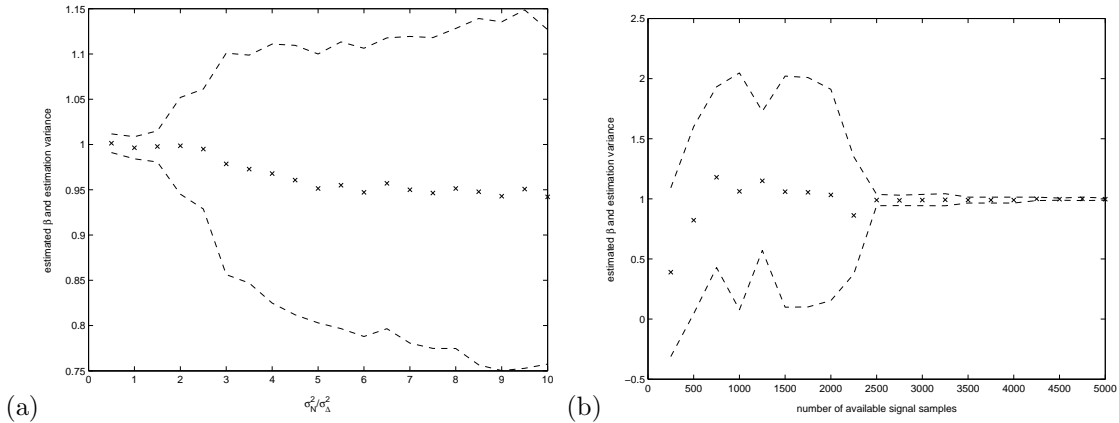


**Figure 6.** Plot of  $\hat{\beta}$  for ML estimation averaged over different audio signals, for fixed  $\beta = 1$ . The crosses represent the estimation mean. The dashed curves represent the variance of the estimation in both directions. (a)  $\frac{\sigma_N^2}{\sigma_\Delta^2}$ , (b) number of available samples.

no periodicity in  $\Phi_X(\omega)$ . Further decreasing  $\alpha$  will cause  $A_{k,W=0}(x)$  and  $A_{k,W=1}(x)$  to overlap. An illustration of these cases is shown in Figure 7.

We can conclude that in the case of large enough number of zeros and ones in the watermark bitstream, the Fourier based approach will work only within the restriction  $\sigma_N^2 < \sigma_\Delta^2$ . The ML approach does not rely on the discontinuity in the PDF of the watermarked data and therefore is invariant to this restriction.

## 7. CONCLUSION

We presented two statistical procedures for estimation of scaling factors in attack channels consisting of amplitude scaling followed by additive noise. The advantage of the procedure based on characteristic functions is that the method relies on the discontinuity of the PDF of the watermarked data, and is not "generally" dependent on the host signal. However, for too strong noise in the attack channel, the method fails. Another disadvantage is the insecurity. An attacker can easily determine the quantity  $\frac{\alpha}{\Delta\beta}$  from the characteristic function of the received data and decode the watermark by directly applying lattice decoding with step size  $\frac{\beta\Delta}{\alpha}$ . The method is computationally cheap and suitable for real-time applications. The second method based on ML estimation is computationally more expensive than the method based on Characteristic functions. This is due to the difficulty in finding an analytical expression for the PDF of the received data, that would allow for an appropriate optimization method<sup>‡</sup>. In our implementation, though, we managed to estimate  $\beta$  in around 50 sec. from 10000 signal samples. Another disadvantage of the method is that it is theoretically dependent on the host signal statistics (although the experimental results indicate good performance in case of model mismatch for a variety of audio host signals). The advantage of the method is the high estimation accuracy even in the presence of very strong noise in the attack channel. In the case of model mismatch, in terms of the ratio  $\frac{\sigma_N^2}{\sigma_\Delta^2}$ , the ML approach gives better results than the Fourier based approach, while in terms of available signal samples, the Fourier based method gives superior estimation. For future work, we plan to do analysis and experiments of the proposed methods in the presence of dither for security purposes.

## REFERENCES

1. P. Moulin and A. O'Sullivan, "Information-Theoretic Analysis of Information Hiding," *IEEE Transactions on Information Theory* **49**, pp. 563–593, March 2003.

<sup>‡</sup>A convenient analytical expression for the PDF of the received data would also allow for a more in depth theoretical analysis of the ML approach (theoretical estimation bias and variance).



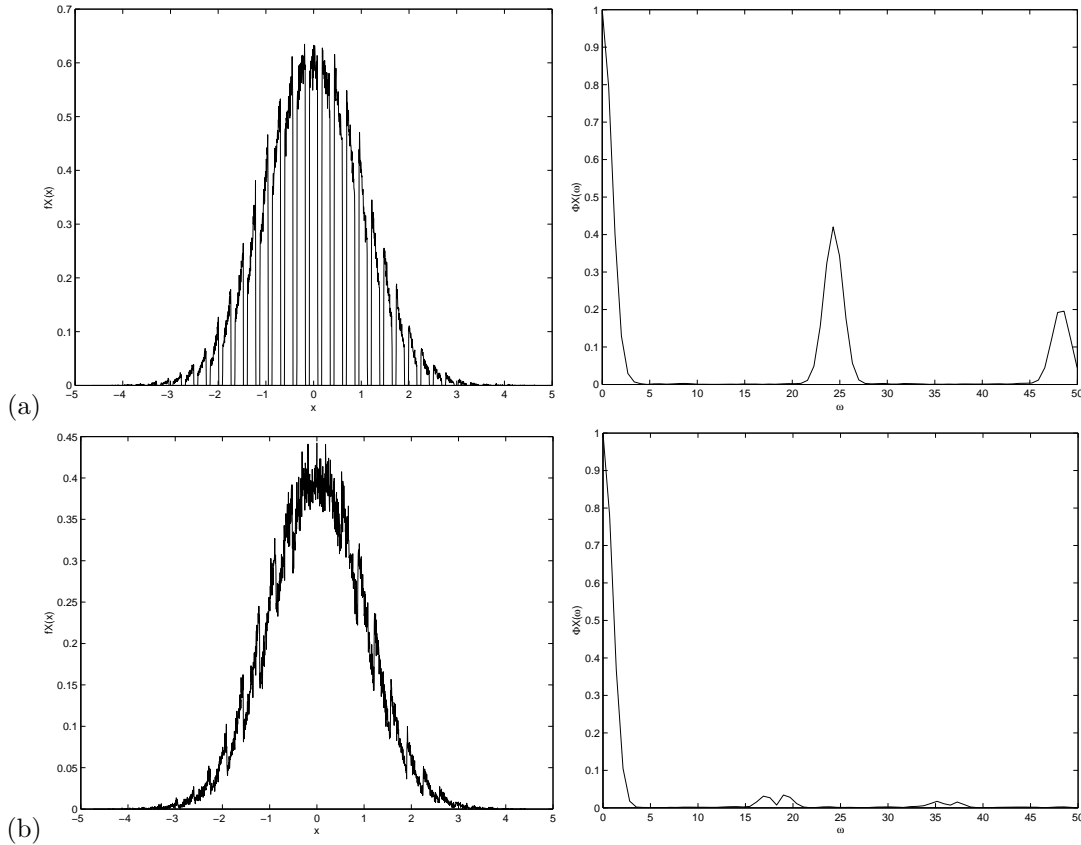


**Figure 7.** Graphs of  $f_X(x)$  and their corresponding  $\Phi_X(\omega)$  in the case of  $P(W = 0) = P(W = 1) = 0.5$ , for different values of the ratio  $\frac{\sigma_N^2}{\sigma_\Delta^2}$ . (a)  $\frac{\sigma_N^2}{\sigma_\Delta^2} = 0.5$ , and (b)  $\frac{\sigma_N^2}{\sigma_\Delta^2} = 1$ .

2. A. S. Cohen and A. Lapidoth, "The Gaussian Watermarking Game," *IEEE Transactions on Information Theory* **48**, pp. 1639–1667, June 2002.
3. J. J. Eggers, R. Bauml, and B. Girod, "Estimation of Amplitude Modifications before SCS Watermark Detection," *SPIE Security and Watermarking of Multimedia Contents* **4675**, pp. 387–398, January 2002. San Jose, CA.
4. P. Moulin and A. Ivanovic, "Nonadditive Gaussian Watermarking and its Application to Wavelet-based Image Watermarking," *IEEE International Conference on Image Processing*, April 2002. Rochester, NY, USA.
5. K. Lee, D. S. Kim, and K. A. Moon, "Amplitude-Modification Resilient Watermarking Based on A-Law Companding," *IEEE International Conference on Image Processing*, September 2003. Barcelona, Spain.
6. M. L. Miller, G. J. Doerr, and J. Cox, "Dirty-Paper Trellis Codes For Watermarking," *IEEE International Conference On Image Processing* **2**, pp. 129–132, September 2002. Rochester, NY.
7. M. Kesal, M. K. Michak, R. Koetter and P. Moulin, "Iteratively Decodable Codes for Watermarking Applications," *Proc. 2nd Int. Symp. on Turbo Codes and Related Topics, Brest, France*, September 2000.
8. M. H. Costa, "Writing on Dirty Paper," *IEEE Transactions on Information Theory* **29**, pp. 439–441, May 1983.
9. J.J. Eggers, J.K. Su and B. Girod, "A Blind Watermarking Scheme Based on Structured Codebooks," *IEE Colloquium: Secure Images and Image Authentication*, April 2000. London, UK.
10. T. Kawata, *Fourier Analysis in Probability Theory*, Academic Press, 1972. page 320.